Scientific Research Publishing

Journal of Power and Energy Engineering, 2022, 10, 90-115
https://www.scirp.org/journal/jpee
ISSN Online: 2327-5901
ISSN Print: 2327-588X

Energy Efficiency Technologies for Hydroelectric Power Plants: A Case Study in Brazil

Thiago Averaldo Bimestre[1*], José Antonio Mantovani Júnior[2], Eliana Vieira Canettieri[1], Celso Eduardo Tuna[1], Pedro Magalhães Sobrinho[1]

[1]Chemistry and Energy Department, School of Engineering, São Paulo State University UNESP, Guaratinguetá, Brazil
[2]Center for Weather Forecasting and Climate Studies, National Institute for Space Research CPTEC/INPE, Cachoeira Paulista, Brazil
Email: *thiagobimestre@hotmail.com

How to cite this paper: Bimestre, T.A., Mantovani Júnior, J.A., Canettieri, E.V., Tuna, C.E. and Sobrinho, P.M. (2022) Energy Efficiency Technologies for Hydroelectric Power Plants: A Case Study in Brazil. *Journal of Power and Energy Engineering*, **10**, 90-115.
https://doi.org/10.4236/jpee.2022.105007

Received: April 15, 2022
Accepted: May 28, 2022
Published: May 31, 2022

Abstract

Hydroelectricity has great importance for the global macroeconomy. In Brazil, hydroelectricity has been highlighted as the main source of generation of the electric system both for its economic competitiveness and for the abundance of this energy resource. Based on a diagnosis methodology, this article presents a case study in a Brazilian hydroelectric plant in order to optimize the use of energy and propose improvements regarding the rationalization of its application. The systems associated with energy generation were evaluated and the results proved to be potentially advantageous with an estimated savings of 2910 MWh/year in the electricity consumption of the installation itself, with better use of the equipment and the possibility of increasing the power generated.

Keywords

Hydropower Plant, Renewable Energy Technology, Energy Efficiency, Energetic Diagnosis, Sustainable

1. Introduction

World energy consumption continues to grow in the past few decades, especially in developing countries. Currently, most of the energy for daily activities is non-renewable, and it has limited resources, *i.e.*, the energy produced from fossil fuels. This context of growing concern over the decreasing abundance of primary energy sources and environmental preservation has led countries to consider other energy resources to ensure the future energy supply-demand. The mitigation of environmental impacts from greenhouse gases is a global challenge that

motivates the international community to introduce new strategies [1], including a greater diversification of the energy matrix with more significant participation of renewable and alternative sources. In this sense, hydroelectricity is recognized as part of renewable technologies, with clean power generation, low costs, and moderated environmental impacts compared to fossil fuels [2] [3] [4] [5] [6].

In 2020, the global hydroelectrical capacity increased 1.6%, reaching 1330 GW, and achieved a record of 4370 TWh of generated clean power [7]. China is the world leader in terms of total installed hydropower capacity with over 370 GW, followed by Brazil (109 GW), the USA (102 GW), Canada (82 GW), and India (50 GW) [7]. Brazil has a predominantly renewable energy matrix with 84.8% of the internal power supply, in which the hydro source accounts for 65.2% of this total given the 12 Brazilian hydrographic basins [8].

Beyond the indicated advantages, hydroelectrical generation technology is flexible and recommended as a baseload for most utilities because it is one of the most economically viable in terms of electricity generation costs [9] ranging from 0.02 US$/kWh to 0.19 US$/kWh [10]. Furthermore, the efficiency of the energy conversion system for a well-operated hydroelectric plant can reach 85% with a high capacity to respond to fluctuations in energy demand [11] when compared to thermoelectric equivalents whose efficiency is generally below 50% [12] [13].

Although studies on hydroelectric plants are considered mature, many plants have been in operation for decades and others are under construction or have already been awarded the operation and maintenance of the various components and systems that make up a hydroelectric plant are critical points for a generation of efficient energy. In this sense, it is necessary to resort to investments with a quick return, mainly in energy savings through management, new technologies, and policies, and regulations.

Thus, the present study seeks to investigate, understand, and explore the processes of a hydroelectric plant focusing on energy use optimization and proposing improvements regarding the rationalization of its application aiming at the energy supply system reliability. Another factor is to comply with the growing demand of the regulatory entity for the system operation without interruptions related to failures.

This study should be understood as an investment in the useful life extension of power plant components, in the reduction of unavailability risks, in the operational simplifications, in reliability increase, and if possible, in the increase of the power generation [14] [15].

2. Hydroelectric Power Plant

The hydroelectrical power plant is in the Rio Claro district at Paraibuna city, São Paulo state, Brazil. The power plant construction began in 1964 and was concluded in 1978 through a consortium among the federal government, the São

Paulo state government, the Rio de Janeiro state government, the Light company, Furnas, and the CESP, which the latter was granted the concession to operate the hydroelectric plant (HP).

The reservoir has a total area of 224 km^2 covering beyond Paraibuna city, the Redenção da Serra and Natividade da Serra cities in the Sao Paulo state. Paraibuna HP has a total installed capacity of 85 MW, operating with two generating units (GU) turbines of the Francis type, promoting the flow regularization of the Paraíba do Sul River and bringing countless energy benefits to the region and Brazil. Among the highest in Brazil, its dam is 104 m high.

Besides the power generation activities, the plant promotes the management of flora and fauna, with sectors of forestry, bird nursery, and fish farming, in addition to promoting environmental education in its projects and lake crossings through ferries, which guaranteed the organization, in 2010, the ISO 9001 Standard.

3. Methodology

The methodological approach is based on data collected from technical visits during 2019, reading maintenance and operation manuals of the equipment, and interviews with operators, employees, and managers of the plant. Only the components of the power generation system are investigated.

3.1. Evaluation of the Open Cooling System of the GU's Combined Bearing

Both generating units GU-1 and GU-2 have a combined bearing cooling system equipped with two shell and tube heat exchangers, two 100 hp engine pumps for oil circulation, piping, and filters. The heat exchangers maintenance is planned to occur without shutting down the generating unit, if a second heat exchanger unit is in reserve, which does not always happen.

In the combined bearing heat exchanger, the oil flows through the shell, and the cooling water flows through the tubes due to is more prone to fouling. Although, the presence of iron-oxidizing bacteria in the raw water reservoir greatly aggravates the situation of the heat exchangers, requiring cleaning at least five to six times a year. In addition, in the open system, 3.6 m^3/min. of raw water from the dam is used for cooling without passing through the turbine.

Experience shows that operating with an open circuit without preventive measures that can reduce the actions of the iron-oxidizing bacteria is not the most appropriate because it is necessary to stop the generating units for cleaning and ensure the integrity of the generator and the bearings.

3.2. Generator Cooling Evaluation

The power generator associated with the turbine is the most complex equipment in its operation due to the numerous stresses suffered by mechanical, electrical, and thermal effects [16]. In this sense, the GU-2 unit cooling system under

full-power operation is evaluated. Table 1 shows the GU's nominal data.

Six closed-circuit airflow measurements were performed in the six air-to-water radiators of GU-2 to study temperature variations. The instrument used was a Tec – Probes Testo N˚445 anemometer. A wooden device was developed by dividing the measurement areas of each exchanger into eighteen quadrants. In each quadrant, five measurements (one at each exchanger tip, and one at the center) were performed using the anemometer.

Experimental measurements of the thermal performance with water flow variations in the cooling circuit were not performed due to the low water level upstream (atypical seasonal condition) and consequent limitation of the turbine flow (active power of approximately 23 MW). Due to this unusual condition, a thermal computer modeling of the generator was developed, applying the original design data, thus seeking information for an adequate evaluation of the cooling conditions and possible limits and operational optimizations of the generator and its cooling system.

Normalized parameters (calculating and operating parameters) are applied to generators modeling. For instance, the standard cold air temperature of 40˚C is a reference temperature to the generator components. All temperature gradients (Δt) computed for any generator component are always added to reference temperature or exchange outlet temperature, and inlet machine temperature. Many components were considered to this modeling such as copper stator, iron stator, and copper rotor, and were estimated following the operating design calculation assumptions, without operational faults. Note that, some typical parameters related to these generators are assumed in the loss-modeling due to unknown real-data values such as electrical conductivity of the stator and rotor covers, as well as the hysteresis, and eddy and Foucault losses in the magnetic plates of the stator core.

3.3. Evaluation of the Sump Water Pumping System

HP drainage sump is elevated at 620.00 m and has dimensions 2.1 m × 2.1 m with 3.0 m of depth. The sump receives the seepage water from the power plant through the existing channels in the galleries, the discharge from the cooling system of the turbine coal seam, and from turbine guide bearings when these

Table 1. Nominal data of generating units.

Unit rated power	42500 W
Rated voltage	13.8 kV
Stator current	2092 A
Excitation voltage	125V
Excitation current	913 A
Number of units	02 (GU1, GU2)
Power ratio	0.85

operate through the open cooling circuit.

The drainage sump design foresees water pumping through three motor pumps installed at 620.00 m elevation and with 4-inch discharge piping with an outlet in the escape channel (downstream). There are three vertical centrifugal engine pumps, each with a capacity of 500 L/min. and a 440 V, 7.5 hp engine.

For the safe operation of the plant in emergencies, a submerged motor pump (flight pump) was installed, with a capacity of 1800 liters per minute and a voltage of 220 Vac. This pump is connected to a 4-inch pipe, as the drainage pumps through a hose, check valve, and gate valve.

Taking advantage of the reservoir's waterfall, a double hydro-ejector is installed, with a calculated flow rate of 1500 L/min. For this, the 4-inch pipe taken from the forced conduit was used, initially planned for the fire-fighting system, and the discharge is interconnected to the 8-inch water hammer piping. However, this hydro-ejector is currently out of operation, and the objective of this study is to size a new hydro-ejector to decrease the electrical energy consumption with the motor pumps. The calculation procedure for hydro-jet sizing is available in Appendix A.

3.4. Efficiency Evaluation of the Forced Air Injection System in the Turbine

The forced air injection system in the turbine is used to mitigate the effect of hydraulic instability (vortex) in the generating units GU-1 and GU-2. In the commissioning test of the generating units, it was found that in the range between 18 and 35 MW there was a large power variation (±10 MW) due to the hydraulic instability (vortex) in the suction tube, even operating with the forced air injection system.

The manufacturer installed a valve coupled to the lower part of the shaft (hollow) near the turbine rotor, which opens and closes by pressure variation to circumvent the issue. When the pressure is low, natural air intake occurs, which attenuates the intensity of the vortex (pressure variation), caused by the center vortex of the turbine rotor, and otherwise, the valve closes. This solution significantly minimized vibrations in the structures, pressure oscillations in the turbine's suction tube/lid, and power oscillations. It is noted that the operating range of the GU-1 and GU-2 was established after the introduction of the natural shaft aeration valve there was no mention of the performance of the forced air injection system. It is also observed that there is no information/documentation on the results of tests carried out after the installation of the natural axle aeration valve, as well as no record of the influence of the natural and forced air injection system on the dynamic behavior of the generating units.

For this reason, a series of tests and measurements with and without forced-air injection was carried out on the GU-2 generating unit to evaluate shaft oscillations, vibrations, pressure pulsations, varying the power within the operating range currently in effect. **Figure 1** shows the current operating range curve of the GU-1 and GU-2.

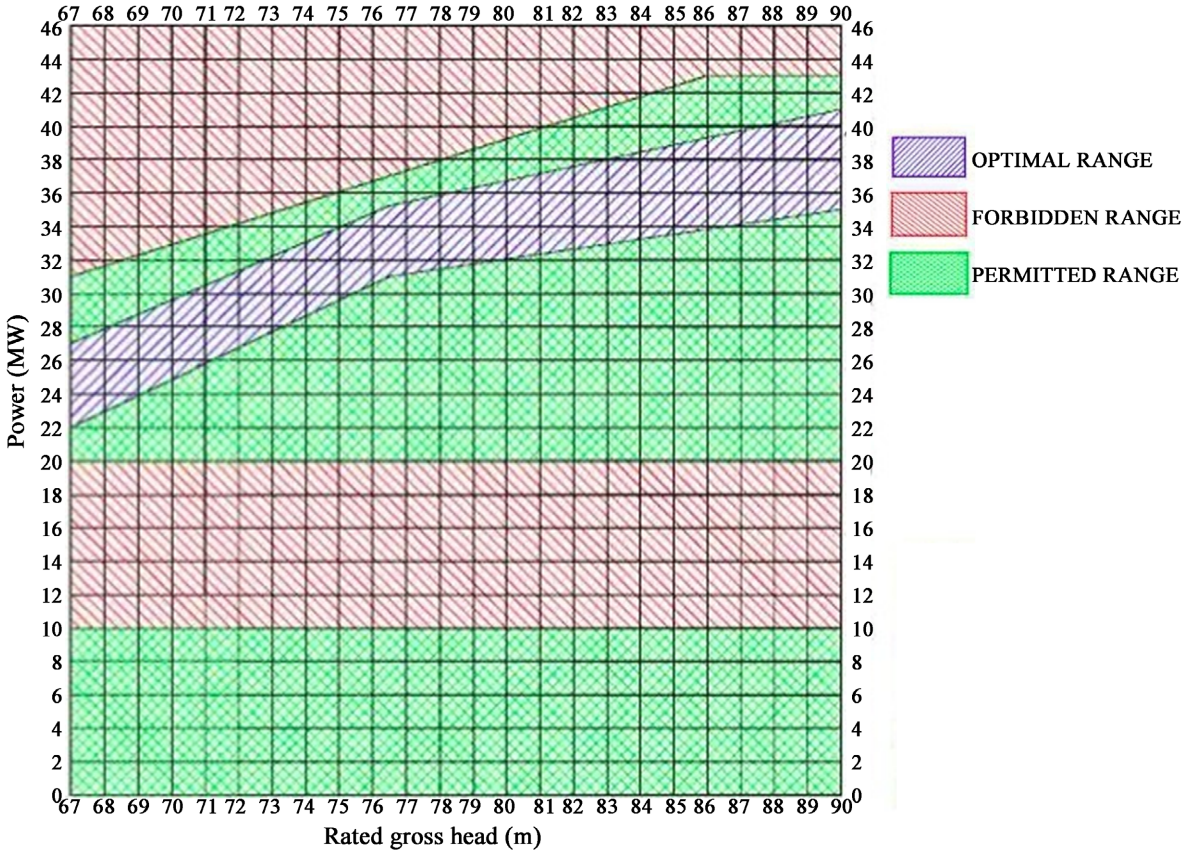

Figure 1. Operational range of GU-1 and GU-2 generating units.

4. Results

Through the surveys carried out on the plant's generation systems and equipment, it was possible to draw up an energy panorama and understand how energy is being used. From this context, it became possible to propose more energy-efficient solutions.

4.1. Closed Cooling Circuit for the Combined Bearing

The installation of a parallel circuit for cooling the oil was proposed, which is interconnected by valves to the open water circuit called the closed water circuit composed of three 40 hp engine pumps for water circulation, plate exchangers cooled with water from the main filters, and the 12 m^3 reservoir fed with mine water (pure). In addition, it was suggested to design a soft starter and selective starting system, with a switching system that eliminates thyristor bridges when the pump reaches the nominal rotation and with an automatic logic that considers independent starts for each pump. The proposed actions are mainly aimed at saving cooling water and energy, reducing downtime for cleaning the heat exchangers, and providing an opportunity to check the capacity of the current emergency diesel set against the instantaneous power required in the case of a black start. Other priority loads for a black start also merit analysis.

With the use of the closed cooling system considering only one stop per year

of 8 hours to change the set of air-water radiators against five stops on average of the open system, it is estimated to save approximately 2600 MWh/year in energy consumption. Still, with the use of pure mine water and considering the nominal water flow rate of the radiators of 3.6 m^3/min., a saving of approximately 2.0 million m^3 of water per year was estimated.

4.2. Generator Cooling System

According to the measurements taken, it appears that the generating unit GU-2 has an airflow rate about 20% higher than the manufacturer's theoretical value. The manufacturer's technical manual informs a total flow rate of 401 m^3/min., while the sum of the measured values reached 488 m^3/min. The generating units have two types of radiators: the finned tube type (tubes with circular fins) and the "compact cooler" type. No significant differences between the two types can be detected from measurements. If there is a need to look deeper into this subject, more sensitive pressure drop measurements (static pressure) between air inlet and outlet should be done, although the measured flow values are higher than expected. On the other hand, it has been observed that many radiators do not have side fittings or side seals that allow preventing the "leakage" of hot air. In other words, a portion of the air is not being cooled, thus losing some of the heat exchange efficiency. It is recommended that a detailed inspection be carried out on them, and the necessary corrections are made. Concerning experimental measurements of thermal performance, it is recommended that some minimum conditions be met:

- The previous cleaning of all air-water heat exchangers ideally always uses pure water free from contamination problems and iron-oxidizing bacteria. Deaeration is suggested after reinstallation and before release for operation;
- Pre-calibration of RTD (Resistance Temperature Detector) temperature reading systems;
- Pre-measurement of the cold ohmic resistance of the rotor winding;
- For the hot resistance measurement of the rotor winding, determine the optimal location for measuring U_{exc} and I_{exc} (excitation voltage and current respectively);
- Having sufficient upstream water level for loading at full load, as well as a schedule that allows sufficient time for the various stages of testing, with adequate temperature stabilizations.
- Have simultaneous water flow measurements. Ideally, it should be on the water inlet pipe. In eventual tests with water flow reduction, it is suggested that it be by the valve on the water outlet pipe.

The theoretical modeling of the generator, with a view to thermal equilibrium conditions, was elaborated based on design data—drawings and the manufacturer's technical manual. **Figure 2(a)** shows the result of the generator modeling with a ventilation system view. The air velocities from different generator points were obtained considering the real dimensions from two channels on the rotor

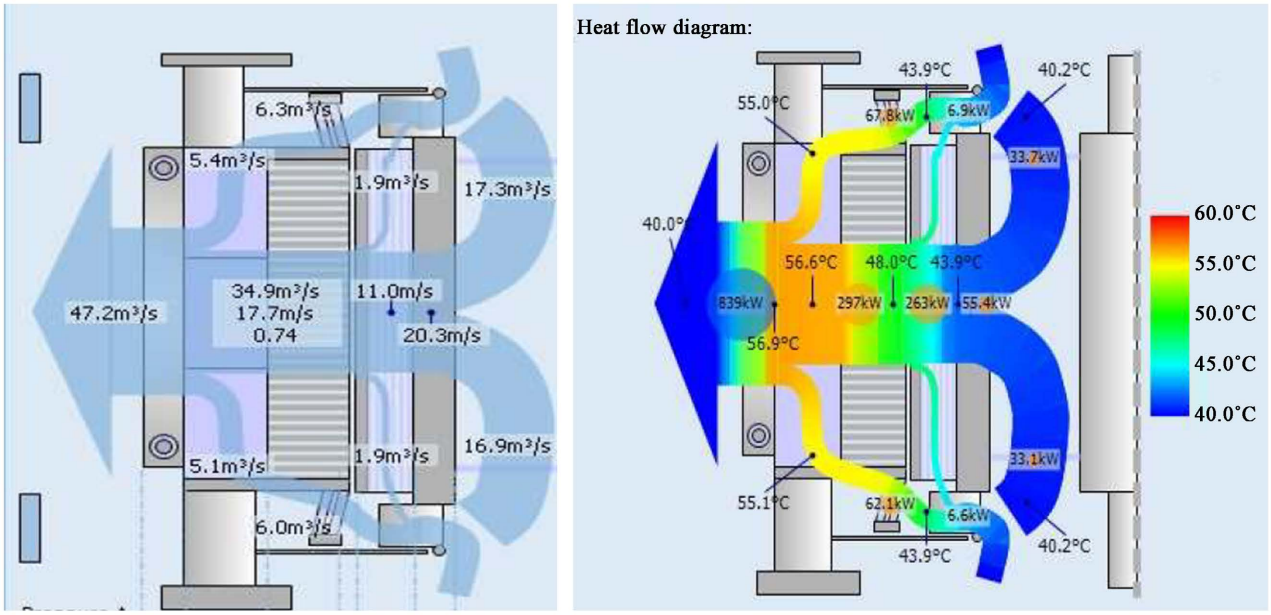

(a) (b)

Figure 2. Ventilation profile for GU-2 in (a) Loss profile, and heating and cooling airflow of the generator at full rated load in (b).

crown providing radial ventilation and the axial ventilation from both upper and lower fans establishing the generator ventilation system.

The airflow rate through the six heat exchangers found by modeling was 47.2 m^3/s. The predicted value through factory design is – 401.2 $m^3/min.$ × 1/60 × 6 (exchangers) = 40.12 m^3/s, which corresponds to about 15% lower compared to the value found in the model. If compared to the measured value in the generator GU-2 – 488 m^3/min × 1/60 × 6 (exchangers) = 48.8 m^3/s, may be concluded that the total value of the measured airflow and the model value is closer. **Figure 2(b)** shows the distribution of computed losses:

- Electromagnetic losses generated in the stator core;
- Joule effect losses were generated in the copper of the stator and rotor windings;
- Additional losses due to scattering fields;
- And the losses by ventilation friction generated by the cooling air itself that circulates in a closed circuit, passing through the rotor crown channels, the winding heads, the air gap, and the stator ventilation ducts, and finally, already hot, through the heat exchangers, to be cooled again.

The diagrams in **Figure 2** are closely interconnected. Both diagrams consider the generator as an adiabatic system (when one does not consider the heat exchanges by convection or irradiation through the generator walls with the external environment) where the circulation air cools all the internally generated heat. The air transfers all the thermal energy from losses to the water circulating through the air-water heat exchangers.

Finally, because of the thermal modeling of the generator, **Table 2** indicates the stabilized temperatures of the generator's parts of interest, considering the nominal operating conditions and the cooling inlet water temperature at 28˚C.

Table 2. Stabilized temperatures of the generator's parts of interest.

Temperatures	T_{abs}	ΔT
Slot RTD (97/95/97)	97˚C	57˚C
Maximum slot copper	110˚C	70˚C
Maximum overhang	108˚C	68˚C
Rotor cooper measured	84˚C	44˚C
Maximum rotor copper	94˚C	54˚C
Maximum stator yoke	69˚C	29˚C

It is important to note that in this theoretical simulation the actual stator copper temperature (110˚C) when the slot RTD reading is at 97˚C, and the stator iron RTD reading is at 69˚C. The 13˚C of Δt between the copper temperature (internally in the bar or coil) and the temperature read at the slot RTD is of special interest and attention when seeking a reduction in life losses of insulating materials.

The measurements and computational modeling performed served as a preliminary evaluation of the performance of the generator cooling system. However, to obtain data that will lead to actions applicable to the system, an important consideration must be made: considering the generator operating at nominal speed and excited at the nominal voltage at no load, the losses generated by ventilation, iron losses in the stator core, and a low Joule effect loss—IR^2 by the excitation current at no load generate almost 50% of the total losses of the generator (without considering the bearings). The other 50% will only be generated when the generator is both synchronized and loaded by the joule effect losses IR^2 in the stator and rotor windings, and the supplementary losses, also due to the currents circulating in the stator winding. In summary, there are two almost equal shares of losses: 50% at non-load and 50% at full load.

Recall that the three losses generated during operation with load: IR^2 stator, IR^2 rotor, and the additional, vary as a quadratic function of the current. Thus, in approximate values, when the generator is at approximately 70% of the nominal current, the additional losses generated will be 50% ($0.7 \times 0.7 \times I^2$) of the total due to loading. Note that due to the thermal inertia of the generator parts, their stabilization temperatures take time to reach.

The above considerations lead us to a first conclusion that the generator doesn't need to receive the total cooling immediately at start-up. The total cooling from the operation start is harmful, and leads to mechanical fatigue, especially in elements containing materials with different thermal expansion coefficients as with the stator winding. Further studies could confirm a possible gain in power generated, depending on the characteristics of the turbine and other components involved. The airflow measurements through the radiators and the modeling revealed the generator's capability to operate colder or generate more power. However, the thermal calculations of the active parts show a relative gap

in absolute temperatures. Since the generator has class F insulation in the stator winding and lowering the temperature will not bring any real significant benefit in terms of increased life expectancy, the most plausible thing to do would be to start a study of a possible increase in generation power.

4.3. Design of Hydro-Ejectors for Pumping Water from the Sump

Table 3 summarizes the main characteristics of the hydro-ejector for draining sump. The calculation and indication of parameters are given in Appendix A.

Figure 3 shows the plot ζ, $\eta = f(\mu)$, based on Table 3.

Table 3. Hydro-ejector calculation for draining sump.

μ	$\frac{H_3 - H_2}{\frac{V_1^2}{2g}}$	$\frac{H_1 - H_3}{\frac{V_1^2}{2g}}$	ζ	η	$\frac{H_1 - H_2}{\frac{V_1^2}{2g}}$	H_1	H_2	H_3
0	0.369	0.544	0.677	-	0.913	84.2	0	34
0.2	0.293	0.599	0.489	0.098	0.892	84.2	2	29
0.4	0.217	0.653	0.332	0.133	0.870	84.2	4	24
0.6	0.163	0.664	0.245	0.147	0.826	84.2	8	23
0.8	0.108	0.675	0.161	0.129	0.783	84.2	12	22
1	0.065	0.675	0.096	0.096	0.740	84.2	16	22
1.2	0.033	0.653	0.050	0.060	0.685	84.2	21	24
1.4	0.003	0.631	0.005	0.007	0.634	84.2	25.7	26

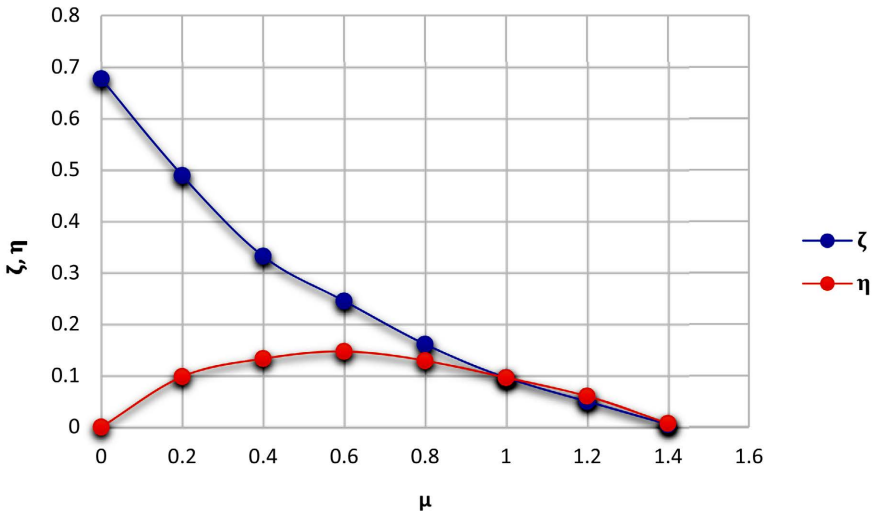

Figure 3. Relation between ζ and $\eta = f(\mu)$.

Given that the pumping flow rate of the planned hydro-ejector is 25 l/s, the commercial values in the standard hydro-ejector pattern were determined at $\emptyset_1$ = 80 mm; at $\emptyset_2$ = 80 mm; at $\emptyset_3$ = 100 mm; a = 135 mm; b = 566 mm; c = 135 mm.

According to the results, the dimensions found are very close to the existing piping in the plant. The results show that the proposal of installing a new hydro-ejector is technically feasible without modifying the configuration of the sump, *i.e.*, using the existing 4" inlet pipe and 8" pipe. Thus, the new main hole hydro-ejector was sized with the capacity to pump all the infiltration water.

Therefore, this proposal could bring savings in energy consumption through engine pumps deactivation estimated at 138 MWh/year and more the maintenance cost since the hydro-ejector for having no moving parts requires almost no maintenance, except routine inspections. The useful life of a stainless-steel hydro-ejector is estimated to be at least fifteen years.

4.4. Forced Air Injection System in the Turbine

4.4.1. Results for Turbine Guide Bearing

In the tested conditions with 0 MW, 5 MW, and 10 MW the shaft wobble measurements at the turbine guide bearing varied from 100 to 200 μm. The shaft wobble measurements at 20 MW, 25 MW, 35 MW, and 40 MW ranged from 100 to 150 μm, but all showed negligible differences whether measured with air or without air. Vibration diagrams are available in Appendix B.

4.4.2. Results for the Suction Tube

In the tested conditions with 0 MW, 5 MW, and 10 MW the maximum pressure oscillation ranged from 300 to 500 mm water column. The maximum pressure oscillation at 20 MW ranges from 250 to 500 mm water column, and at 25 MW the pressure oscillation ranged from 120 to 230 mm water column. The maximum pressure oscillation at 35 MW ranged from 50 to 75 mm water column, and at 40 MW the pressure oscillation ranged from 80 mm water column with air and 150 mm water column without air, but in all of them, the differences measured with air or without air are negligible.

4.4.3. Results for Turbine Cover

In the test conditions with 0 MW, 5 MW, and 10 MW the maximum pressure oscillation was around 0.9 mm/s. In the tested conditions of 20 MW and 25 MW, the maximum pressure oscillation was around 0.55 mm/s and in both conditions of 25 MW and 40 MW the maximum pressure oscillation was around 0.5 mm/s, but in all of them the differences both measured with air and without air are not very significant.

The tests carried out were performed according to the standard for assessing the operating range, which permits verifying the operating range of the generating units is satisfactory. Another finding is the forced injection system contributes very little to improve the dynamic behavior of the generating units. In the tests carried out the performance of the air injection system by the shaft was not planned to verify, but to prove the degree of efficiency is suggested to carry out new tests with and without the aeration valve installed on the shaft.

Although the effect of hydraulic instability interferes very little with the level

of oscillation of the shaft near the combined bearing is important to make this measurement for analysis of the operating range. The maintenance history reveals that the aeration valve is reliable since no serious problems have occurred due to its working pressure of up to 9.0 bar. What is known is that the aeration valve has been stalling in the open position due to the presence of iron-oxidizing bacteria and mud, and when stopped by level variation downstream it provides water leakage through the top of the shaft, wetting the generator. As a proposal, a study to install this valve on the upper part of the shaft next to the collector ring and make a duct to collect the water resulting from the leakage and extend it to a safe place was suggested. The proposal is hard due to the need to protect the generator's excitation bus, which passes through the shaft.

The analyses performed so far show that the dynamic behavior of the generating units operating with forced air injection in the 0 to 10 MW and 20 to 40 MW ranges is not very significant, as verified in the tests performed. It was also observed that there are no restrictions that could impair the turbine performance, such as cavitation, cracks in the turbine's rotor blades, improper sensor actuation, broken piping, or other dynamic problems. Thus, the new suggested operating range would be established as follows: from 0 MW to 10 MW and 20 MW to 40 MW—normal operation, and from 10 MW to 20 MW—prohibited operation.

In addition, the measures listed above would bring significant gains with the deactivation of the air compressors. The stabilization air compressors are of the screw type (40 hp - 440 V - 3.44 m^3 /min - 10 atm) and start operating automatically from a given distributor opening or can be operated manually according to the generation ranges of the generating units. Air is injected into the turbine to dampen the vortex effect on the turbine cover to ensure smoother operation at part load.

Two compressors are operating at full load, each one working together with the generating unit, *i.e.*, the number of hours the compressors have been running is practically the same as the generating units. These two deactivated compressors can replace the general service compressors of the alternative type, which have been in operation for a long time and need maintenance more frequently. The savings would be 172 MWh/year in energy consumption. For these reasons, the promising proposal is indicated to eliminate the operation of the forced air injection system.

5. Conclusion

Energy is a fundamental input to ensuring the country's economic and social development. The rationalization of its use presents itself as a low-cost alternative with a short implementation period. The proposed modifications to the plant's generation systems have shown to be potentially advantageous with an estimated economy of 2910 MWh/year in energy consumption, the better use of equipment, and the gain possibility in generated power. The downtime minimi-

zation, the minimal inventory of spare parts, the elimination of the replacement of parts in good conditions, and the adequacy of the labor force in the interventions are also added.

Availability of Data and Materials

The data supporting the conclusions are included in Appendix A and Appendix B.

Funding

This study was financed in part by the Coordenação de Aperfeiçoamento de Pessoal de Nível Superior—Brasil (CAPES)—Finance code 001.

Conflicts of Interest

The authors declare no conflicts of interest regarding the publication of this paper.

References

[1] Dos Santos, M.A., Damazio, J.M., Rogerio, J.P., Amorim, M.A., Medeiros, A.M., Abreu, J.L.S., Maceira, M.E.P., Melo, A.C. and Rosa, L.P. (2017) Estimates of GHG Emissions by Hydroelectric Reservoirs: The Brazilian Case. *Energy*, **133**, 99-107. https://doi.org/10.1016/j.energy.2017.05.082

[2] Raupp, I. and Costa, F. (2021) Hydropower Expansion Planning in Brazil-Environmental Improvements. *Renewable and Sustainable Energy Reviews*, **152**, Article ID: 111623. https://doi.org/10.1016/j.rser.2021.111623

[3] Koch, F.H. (2001) Hydropower–Internalised Costs and Externalised Benefits. *Externalities and Energy Policy*: *The Life Cycle Analysis Approach*, **15**, 131-139.

[4] Kaygusuz, K. (2009) The Role of Hydropower for Sustainable Energy Development. *Energy Sources*, *Part B*, **4**, 365-376. https://doi.org/10.1080/15567240701756889

[5] Bartle, A. (2002) Hydropower Potential and Development Activities. *Energy Policy*, **30**, 1231-1239. https://doi.org/10.1016/S0301-4215(02)00084-8

[6] Frey, G.W. and Linke, D.M. (2002) Hydropower as a Renewable and Sustainable Energy Resource Meeting Global Energy Challenges in a Reasonable Way. *Energy Policy*, **30**, 1261-1265. https://doi.org/10.1016/S0301-4215(02)00086-1

[7] HA (2021) 2021 Hydropower Status Report. International Hydropower Association. https://www.hydropower.org/publications/2021-hydropower-status-report

[8] Balanço Énergétique Nacional (2021) Ano base 2020/Empresa de Pesquisa Énergétique. Rio de Janeiro, EPE.

[9] USA Department of Energy, Hydropower Technology Information (2012) Basic Energy Information. https://www.energy.gov/eere/water/hydropower-program

[10] Brown, A., Müller, S. and Dobrotkova, Z. (2011) Renewable Energy: Markets and Prospects by Technology. IEA Information Paper.

[11] International Renewable Energy Agency (IRENA) (2012) Renewable Energy Technologies: Cost Analysis Series. Volume 1: Power Sector. IRENA Working Paper 3/5.

[12] Kaunda, C.S., Kimambo, C.Z. and Nielsen, T.K. (2012) Hydropower in the Context of Sustainable Energy Supply: A Review of Technologies and Challenges. *Interna-*

tional Scholarly Research Notices, **2012**, Article ID: 730631. https://doi.org/10.5402/2012/730631

[13] Espinel, A., Díaz, I. and Vega, A. (2021) Distributed Electrical Resources with Micro Hydroelectric Power Plants in Colombia—Study Case. *Energy Reports*, **7**, 169-176. https://doi.org/10.1016/j.egyr.2021.08.059

[14] Abdelaziz, E.A., Saidur, R. and Mekhilef, S. (2011) A Review on Energy Saving Strategies in Industrial Sector. *Renewable and Sustainable Energy Reviews*, **15**, 150-168. https://doi.org/10.1016/j.rser.2010.09.003

[15] Costa, F.S., Raupp, I.P., Damázio, J.M., Pires, S.H.M., Garcia, K., Matos, D.F., Menezes, P.C., Mollica, A.M. and Paz, L.R. (2009) A Decision Support System to Assist River Basin Hydroelectric Inventory Studies in Brazil. In *Water Resources Management* V. *Proceedings of the Fifth International Conference on Sustainable Water Resources Management*, Milan, 20-28 June 2022, 353-365. https://doi.org/10.2495/WRM090321

[16] Pohekar, S.D. and Ramachandran, M. (2004) Application of Multi-Criteria Decision Making to Sustainable Energy Planning—A Review. *Renewable and Sustainable Energy Reviews*, **8**, 365-381. https://doi.org/10.1016/j.rser.2003.12.007

Appendix A. Hydro-Ejectors Sizing

Figure A1 shows a hydro-ejector setup, and a hydro-ejector calculation methodology is defined from it.

Bernoulli equations are applied to reducer calculation, given as follows:

$$\rho \cdot g \cdot H_1 = P_{10} + \frac{\rho}{2} V_1^2 \tag{A1a}$$

$$\rho \cdot g \cdot H_1 = P_1 + \frac{\rho}{2} V_1^2 \tag{A1b}$$

$$\rho \cdot g \cdot H_2 = P_2 + \frac{\rho}{2} V_2^2 \tag{A1c}$$

$$\frac{\rho}{2} \cdot V_1^2 \ll P_1$$

$$\frac{\rho}{2} \cdot V_2^2 \ll P_2$$

$$\frac{\rho}{2} \cdot V_3^2 \ll P_3$$

$$\rho \cdot g \cdot H_3' = P_3' + \frac{\rho}{2} V_3^2$$

or

$$\rho \cdot g \cdot \left(H_3' - H_2\right) = P_3' - P_2 + \frac{\rho}{2}\left(V_3'^2 - V_2^2\right)$$

$$\rho \cdot g \cdot \left(H_1 - H_3'\right) = P_1 - P_3' + \frac{\rho}{2}\left(V_1'^2 - V_3^2\right)$$

Non-considering losses, Equation (A2) is obtained

$$\frac{H_3' - H_2}{H_1 - H_3'} = \frac{P_3' - P_2 + \frac{\rho}{2}\left(V_3'^2 - V_2^2\right)}{P_1 - P_3' + \frac{\rho}{2}\left(V_1'^2 - V_3^2\right)} = \zeta' \tag{A2}$$

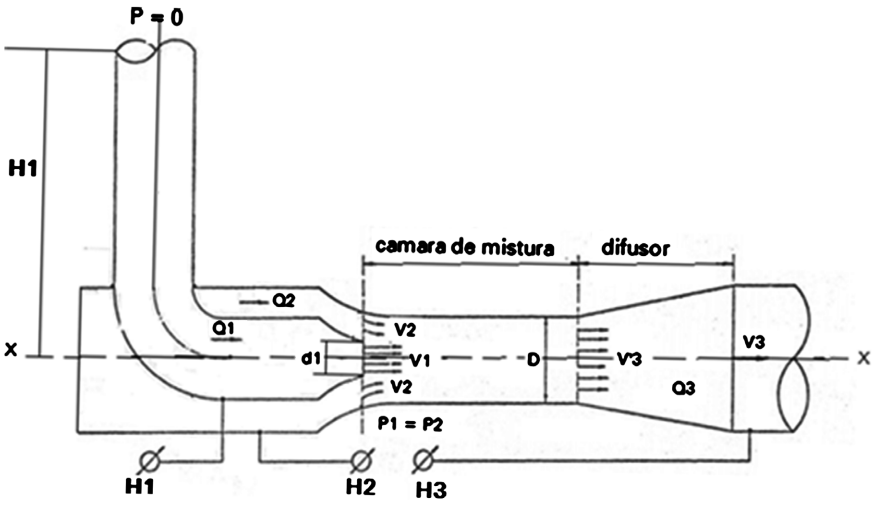

Figure A1. Hydro-ejector setup.

Considering the impulse theorem represented by Equation (A3), that is:

$$\vec{F} = \oint \vec{V} \cdot \rho \cdot \vec{V} \cdot \mathrm{d}\vec{A} \cdot F \tag{A3}$$

$$\left(P_1 - P_3'\right) \cdot A_3' = \rho \cdot A_3' \cdot V_3'^2 - \rho \cdot A_1 \cdot V_1^2 - \rho \cdot A_2 \cdot V_2^2$$

$$\zeta' = \frac{H_3' - H_2}{H_1 - H_3'} = \rho \cdot A_1 \cdot V_1^2 \cdot \frac{P_3' - P_2 + \frac{\rho}{2}\left(V_3'^2 - V_2^2\right)}{P_1 - P_3' + \frac{\rho}{2}\left(V_1'^2 - V_3^2\right)}$$

$$\left(P_1 - P_3'\right) = \rho \cdot V_3'^2 - \rho \cdot \frac{A_1}{A_3'} \cdot V_1^2 - \rho \cdot \frac{A_2}{A_3'} \cdot V_2^2$$

Thus,

$$\left(P_1 - P_3'\right) = -\rho \cdot V_3'^2 + \rho \cdot \frac{A_1}{A_3'} \cdot V_1^2 + \rho \cdot \frac{A_2}{A_3'} \cdot V_2^2$$

Hence,

$$\zeta' = \frac{-\rho \cdot V_3'^2 + \rho \cdot \frac{A_1}{A_3'} \cdot V_1^2 + \rho \cdot \frac{A_2}{A_3'} \cdot V_2^2 + \frac{\rho}{2}\left(V_3'^2 - V_2^2\right)}{\rho \cdot V_3'^2 - \rho \cdot \frac{A_1}{A_3'} \cdot V_1^2 - \rho \cdot \frac{A_2}{A_3'} \cdot V_2^2 + \frac{\rho}{2}\left(V_1'^2 - V_3^2\right)}$$

Let

$$\frac{A_1}{A_3'} = a_1 \text{ and } \frac{A_2}{A_3'} = a_2$$

Normalizing with $\frac{\rho}{2} \cdot V_1^2$ yields

$$\zeta' = \frac{\frac{-\rho \cdot V_3'^2}{\frac{\rho}{2}V_1^2} + \frac{\rho \cdot a_1 \cdot V_1^2}{\frac{\rho}{2}V_1^2} + \frac{\rho \cdot a_2 \cdot V_2^2}{\frac{\rho}{2}V_1^2} + \frac{\frac{\rho}{2} \cdot V_3'^2}{\frac{\rho}{2}V_1^2} - \frac{\rho \cdot V_2^2}{\frac{\rho}{2}V_1^2}}{\frac{\frac{\rho}{2} \cdot V_1^2}{\frac{\rho}{2}V_1^2} - \frac{\rho \cdot a_1 \cdot V_1^2}{\frac{\rho}{2}V_1^2} + \frac{\rho \cdot a_2 \cdot V_2^2}{\frac{\rho}{2}V_1^2} + \frac{\frac{\rho}{2} \cdot V_1^2}{\frac{\rho}{2}V_1^2} - \frac{\frac{\rho}{2} \cdot V_3'^2}{\frac{\rho}{2}V_1^2}}$$

$$\zeta' = \frac{-2\left(\frac{V_3'}{V_1}\right)^2 + 2a_1 + 2a_2\left(\frac{V_2}{V_1}\right)^2 + \left(\frac{V_3'}{V_1}\right)^2 - \left(\frac{V_2}{V_1}\right)^2}{2\left(\frac{V_3'}{V_1}\right)^2 - 2a_1 + 2a_2\left(\frac{V_2}{V_1}\right)^2 + 1 - \left(\frac{V_3'}{V_1}\right)^2}$$

$$\zeta' = \frac{2a_1 + 2a_2\left(\frac{V_2}{V_1}\right)^2 - \left(\frac{V_3'}{V_1}\right)^2 - \left(\frac{V_2}{V_1}\right)^2}{\left(\frac{V_3'}{V_1}\right)^2 - 2a_1 + 2a_2\left(\frac{V_2}{V_1}\right)^2 + 1}$$

$$\zeta' = \frac{2a_1 + \left(2a_2 - 1\right)\left(\frac{V_2}{V_1}\right)^2 - \left(\frac{V_3'}{V_1}\right)^2}{1 - 2a_1 + 2a_2\left(\frac{V_2}{V_1}\right)^2 - \left(\frac{V_3'}{V_1}\right)^2}$$

Considering the losses in the mixing chamber and the diffuser, thus:

$$\zeta' = \frac{\Delta H}{\frac{\rho}{2}V_1} = \varepsilon \frac{\frac{\rho}{2}\cdot V_3'}{\frac{\rho}{2}V_1^2} = \varepsilon\left(\frac{V_3'}{V_1}\right)^2$$

$$\zeta' = \frac{H_3' - \Delta H - H_2}{H_1 - \left(H_3' - \Delta H\right)} = \frac{H_3 - H_2}{H_1 - H_3}$$

$$\zeta' = \frac{2a_1 + \left(2a_2 - 1\right)\left(\frac{V_2}{V_1}\right)^2 - \left(\frac{V_3'}{V_1}\right)^2 \cdot \left(1+\varepsilon\right)}{1 - 2a_1 + 2a_2\left(\frac{V_2}{V_1}\right)^2 + \frac{V_3'}{V_1}\cdot\left(1+\varepsilon\right)}$$

Equation (A4) represents the continuity equation and gives:

$$\frac{V_2}{V_1} = \frac{m_1}{m_2}\cdot\frac{a_1}{a_2} = \mu\cdot\frac{a_1}{a_2} \text{ and } \frac{V_3'}{V_1} = \frac{m_3}{m_1}\cdot a_1 = \frac{m_1 + m_2}{m_1}\cdot a_1 = \left(1+\mu\right)\cdot a_1 \quad \text{(A4)}$$

Thus,

$$\zeta' = \frac{2a_1 + \left(2a_2 - 1\right)\mu^2\left(\frac{a_1}{a_2}\right)^2 - \left(1+\varepsilon\right)\cdot\left(1+\mu\right)^2\cdot a_1^2}{1 - 2a_1 + 2a_2\cdot\mu^2\cdot\left(\frac{a_1}{a_2}\right)^2 + \left(1+\varepsilon\right)\left(1+\mu\right)^2\cdot a_1}$$

The yield is given by Equation (A5)

$$\eta = \frac{m_2\left(H_3 - H_2\right)}{m_1\left(H_1 - H_3\right)} = \mu\cdot\zeta \quad \text{(A5)}$$

Then, from the following characteristics of the hydro-ejector:

$$\zeta' = \frac{H_3 - H_2}{H_1 - H_3} = f\left(\mu\right) \text{ and } \eta = f\left(\mu\right)$$

Figure A2 shows the new hydro-ejector setup and pipes that must be used.

Surveyed data:

Pressure upstream of the ejector can be calculated using Equation (A6):

$$H_1 = \text{pressure} + \text{level difference} - \text{pressure drop} \quad \text{(A6)}$$

$$H_1 = 10.0 + \left(694.60 - 620.00\right) - 0.3$$

$$H_1 = 10.0 + 74.60 \text{ metros} - 0.4 = 84.2 \text{ m } H_2O$$

Pressure in the suction chamber can be calculated using Equation (A7):

$$H_2 = \text{pressure} + \text{level difference} - \text{pressure drop} \quad \text{(A7)}$$

$$H_2 = 10.0 - \left(620.0 - 617.0\right) - 0.06 = 6.94 \text{ m } H_2O$$

Pressure at the diffuser outlet can be calculated from Equation (A8):

$$H_3 = \text{pressure} + \text{level difference} - \text{pressure drop} \quad \text{(A8)}$$

$$H_3 = 10.0 + \left(628.70 - 620.0\right) - 0.06 = 18.10 \text{ m } H_2O$$

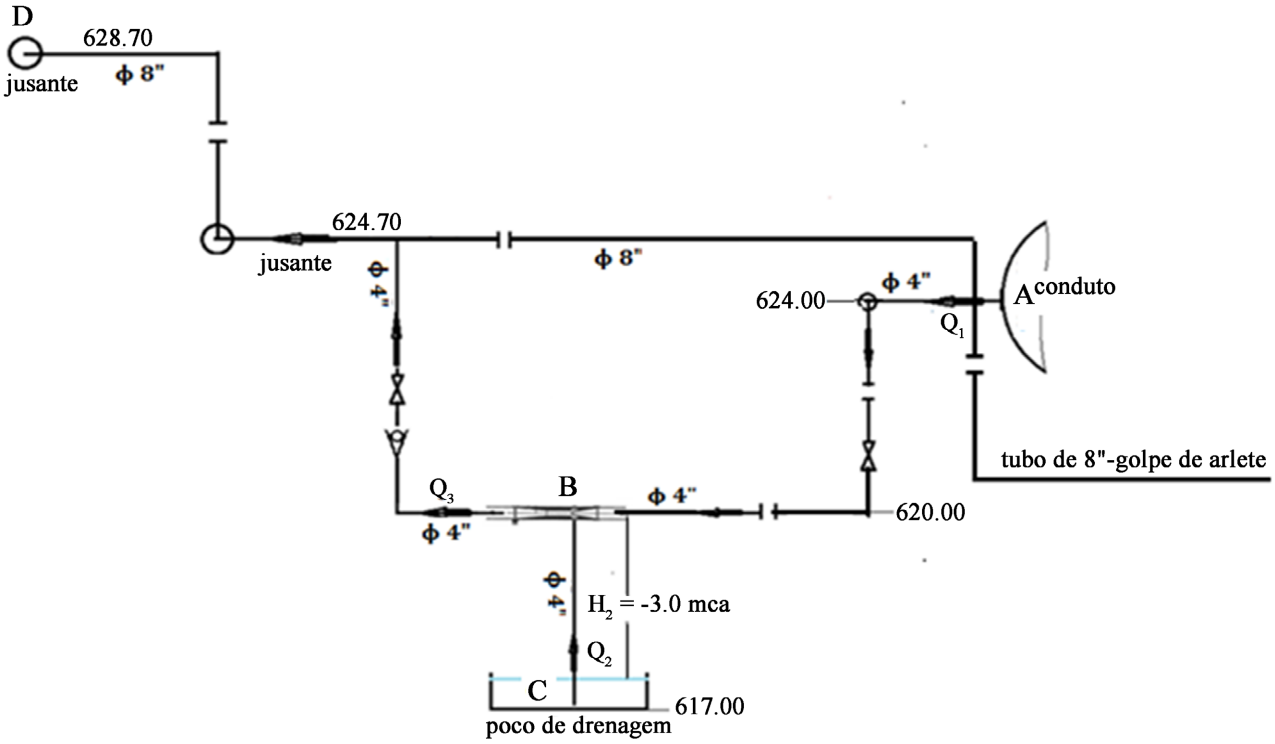

Figure A2. Pumping circuit with hydro-ejector.

Data:

d_1 = pressure tube diameter: 100 mm;

d_3 = discharge tube diameter: 100/200 mm;

Required flow rate Q_2 = 1500 L/min.

Assuming:

$$a_1 = \frac{A_1}{A_3'} = \left(\frac{d_1}{D}\right) = 0.34 \text{ and } A_2 = A_3' - A_1$$

$$a_1 + a_2 = 1.0 = \left(\frac{A_2}{A_3'}\right) = \left(\frac{d_2}{D}\right) = 0.66$$

(Without considering the thickness of the walls)

$$a_1 + a_2 = 1.0 = \frac{A_3}{A_3'}$$

(Mixing chamber section)

With

$$H_1 = 84.2 \text{ m } H_2O$$

$$\frac{p_1}{\rho \cdot g} = -8 \text{ m (without cavitation)}$$

$$\frac{V_1^2}{2 \cdot g} = 84.2 + 8 = 92.2 \text{ m}$$

$$V_0 = \varphi\sqrt{2 \cdot g \cdot H} = 0.95\sqrt{20 \times 92.2} = 40.8 \text{ m/s}$$

Now, assuming $\frac{Q_2}{Q_1} = \frac{m_2}{m_1} = 0.60$ (for $\eta = \max.$)

was found $Q_2 = 90.000\ \text{L/h} = 0.025\ \text{m}^3/\text{s}$, then:

$$\frac{0.025}{Q_1} = 0.60$$

where

$$Q_1 = 0.042\ \text{m}^3/\text{s} \quad \text{but,}$$

$$Q_1 = V_1 A_1 = V_1 \frac{\pi d_1^2}{4} = 38.6 \cdot \frac{\pi d_1^2}{4} = 0.042\ \text{m}^3/\text{s}$$

m^3/s

where

$$d_1 = 37.2\ \text{mm}$$

$$\text{and} \quad a_1 = 0.34 = \frac{A_1}{A_3'} = \left(\frac{d_1}{D}\right)^2$$

was found

$$D = 63.8\ \text{mm}$$

$$\frac{A_2}{A_3'} = \left(\frac{d_2}{D}\right)^2 = 0.66$$

$$d_2 = \sqrt{D^2 \cdot 0.66} = 52\ \text{mm}$$

then, d_1 = 37.2 mm; d_2 = 52 mm and D = 64 mm, values lower than the existing dimensions (pipes).

Table A1 shows the hydro-ejector models developed by JMP-Equipamentos

Table A1. Hydro-ejector types and dimensions.

Model	Ø₁ mm	Ø₂ mm	Ø₃ mm	*a* mm	*b* mm	*c* mm	Weight kg	Max. Flow l/s
1	8	8	10	34	110	32	1.5	0.08
2	10	10	15	34	110	32	1.5	0.21
3	15	15	20	34	110	32	1.5	0.43
4	20	20	25	41	152	37	2.5	0.77
5	25	25	40	52	206	47	5	2.2
6	40	40	50	65	282	56	8	4.3
7	40A	40	50	100	297	100	32	4.9
8	50	50	80	125	404	125	40	13.8
9	80	80	100	135	566	135	52	23.6
10	100	100	150	165	783	165	76	57
11	150	150	200	220	1133	220	140	110
12	200	200	250	280	1469	280	187	196
13	250	250	300	330	1815	330	210	318
14	300	300	380	360	2248	380	290	628

a Jato Engenharia e Comércio Ltda. that can be used as an orientation in similar projects, as well as be used to build larger ones.

Figure A3 shows geometric dimensions of the hydro-ejector models developed by JMP.

Considering that the pumping flow of the hydro-ejector foreseen is 25 l/s, Table A1 points out that the most adequate hydro-ejector would be model 09.

Model 9 dimensions:

Φ_1 = 80 mm;

Φ_2 = 80 mm;

Φ_3 = 100 mm; a = 135 mm; b = 566 mm; c = 135 mm.

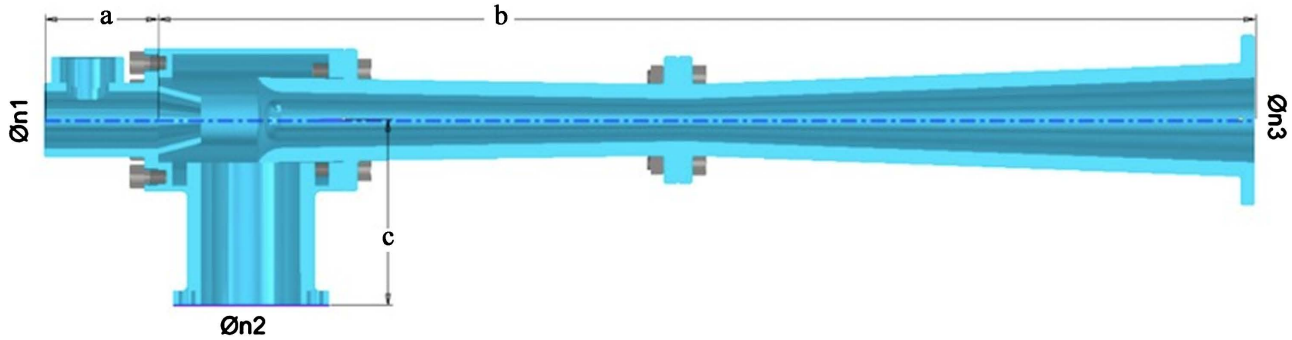

Figure A3. Shows the hydro-ejector with its dimensions.

Appendix B. Forced Air Injection System in the Turbine

Figure B1 illustrates the shaft oscillations with 0, 5 and 10 MW with and without air.

Figure B2 illustrates the shaft oscillations with 20 and 25 MW with and without air.

Figure B3 illustrates the shaft oscillations with 35 and 40 MW with and without air.

Figure B4 illustrates pressure oscillation measurements with 0, 5 and 10MW with and without air.

Figure B5 illustrates pressure oscillation measurements with 20 and 25MW with and without air.

Figure B6 illustrates pressure oscillation measurements with 35 and 40MW with and without air.

Figure B7 illustrates the vibration measurements with 0, 5 and 10MW with and without air.

Figure B8 illustrates the vibration measurements with 20 and 25MW with and without air.

Figure B9 illustrates the vibration measurements with 35 and 40MW with and without air.

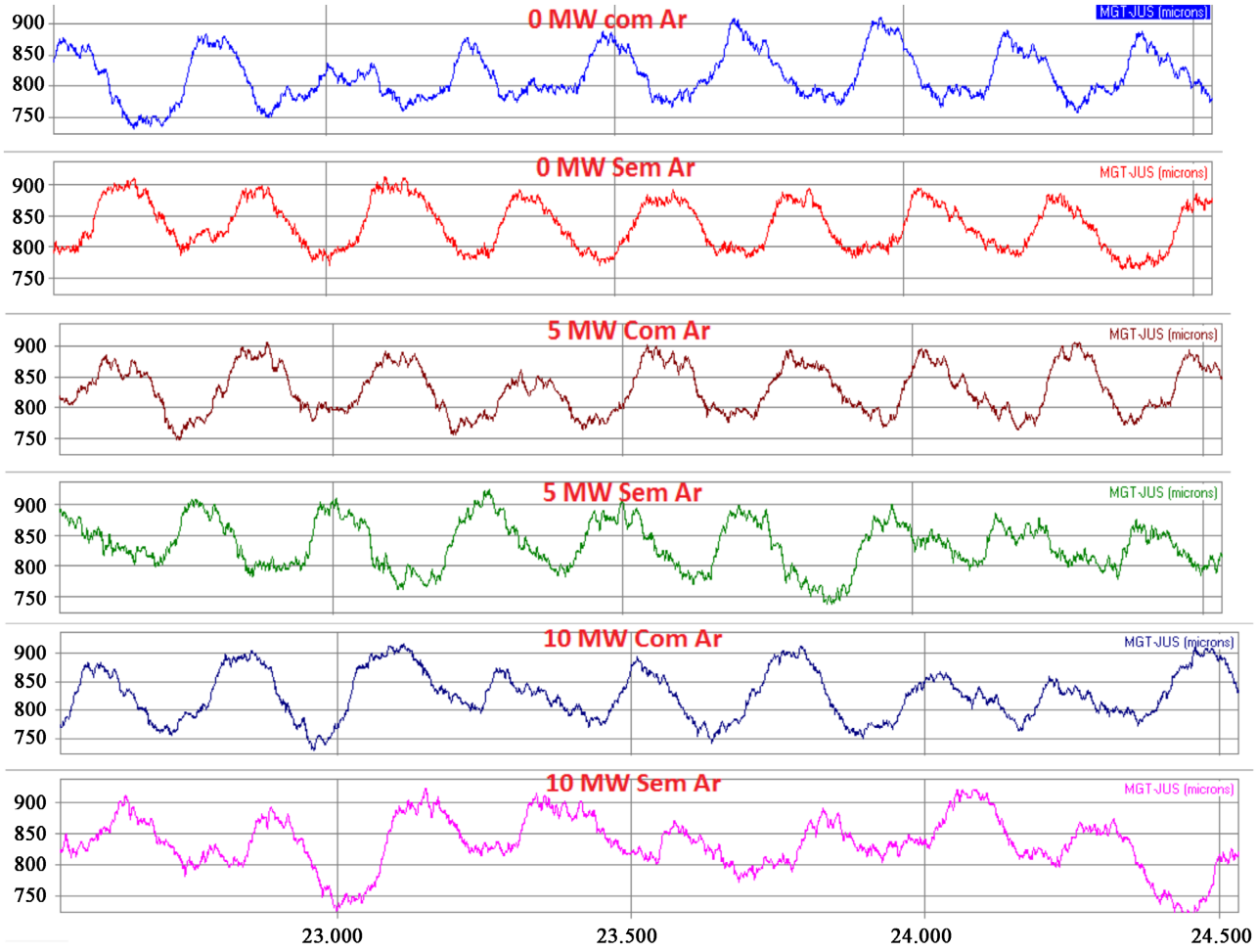

Figure B1. Turbine Guide Bearing—Shaft oscillation measurements with 0, 5 and 10 MW.

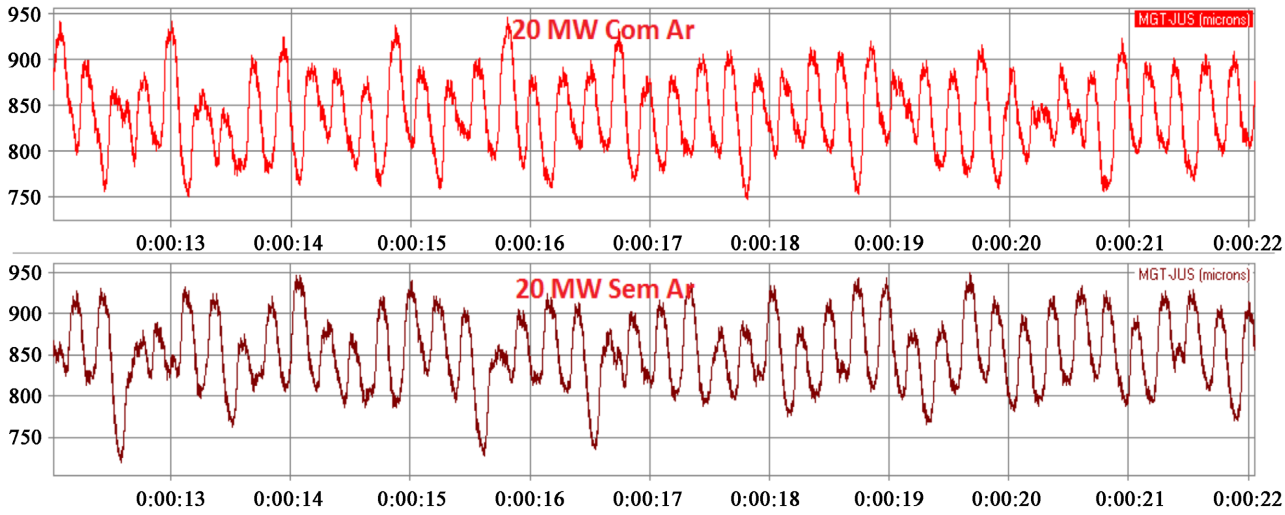

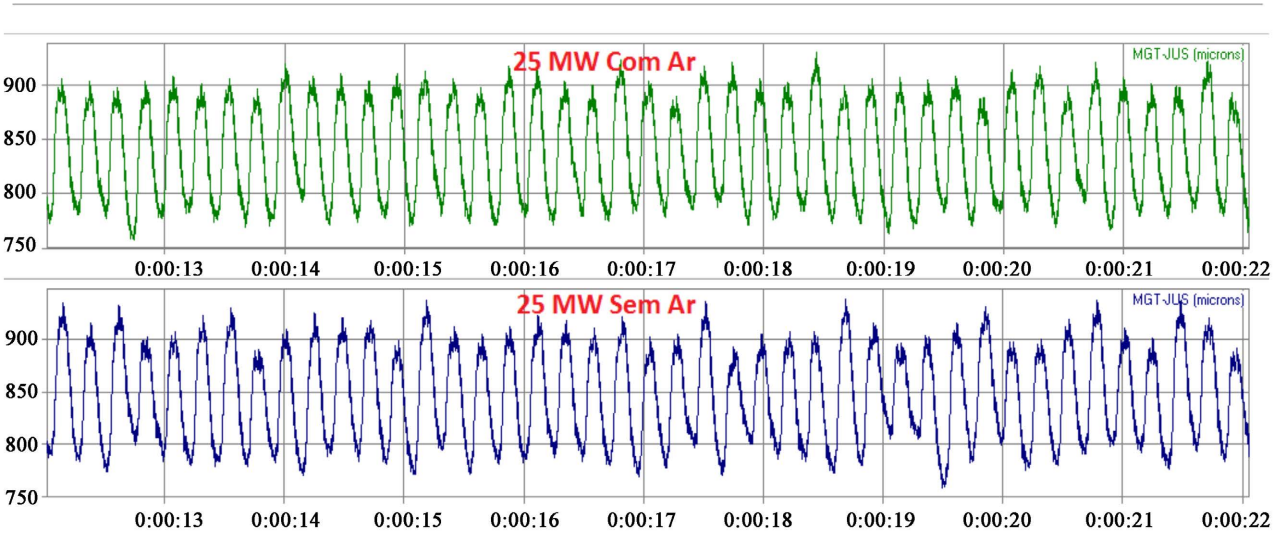

Figure B2. Turbine Guide Bearing—Shaft oscillation measurements with 20 and 25 MW.

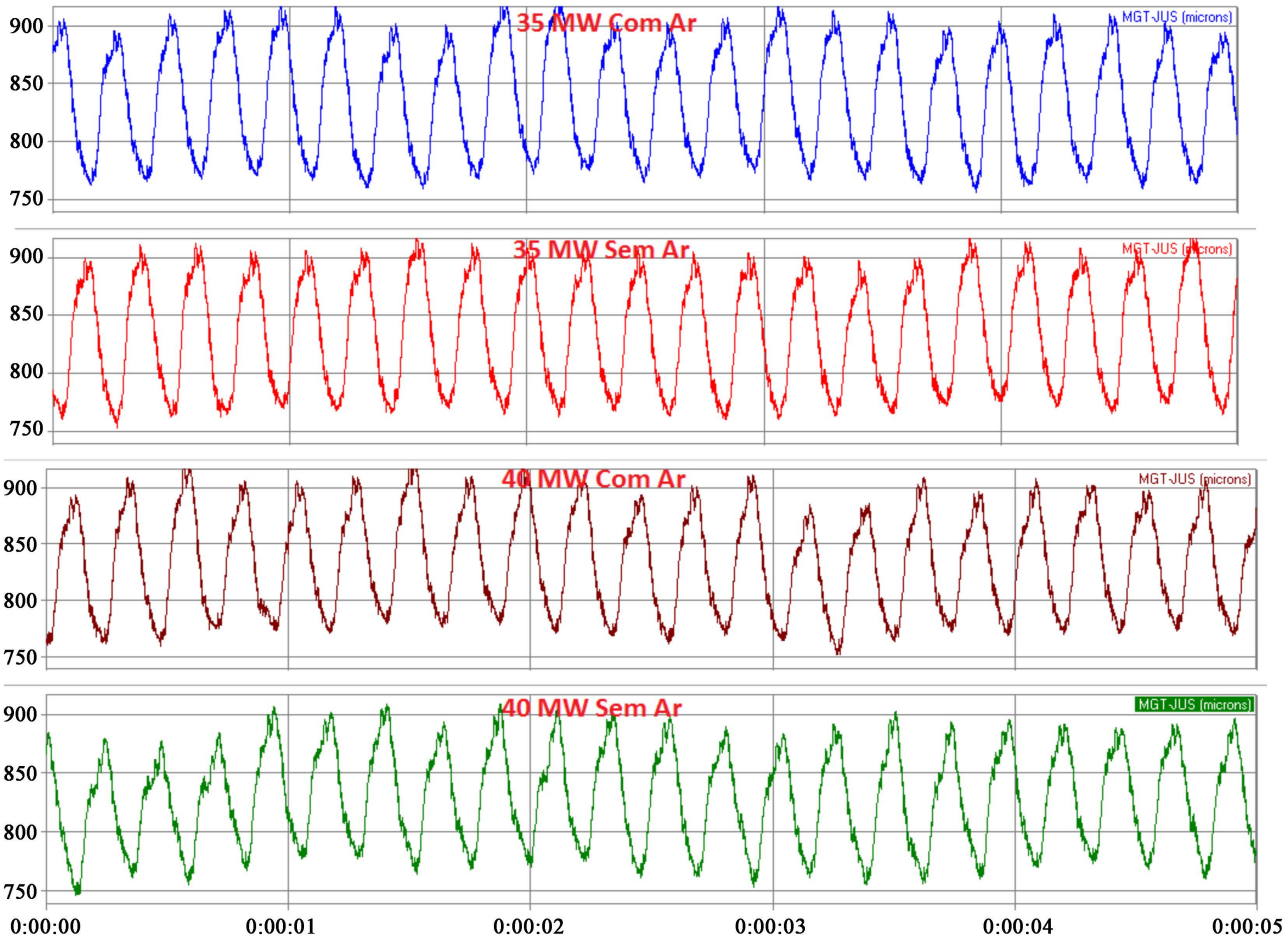

Figure B3. Turbine Guide Bearing—Shaft oscillation measures 35 and 40 MW.

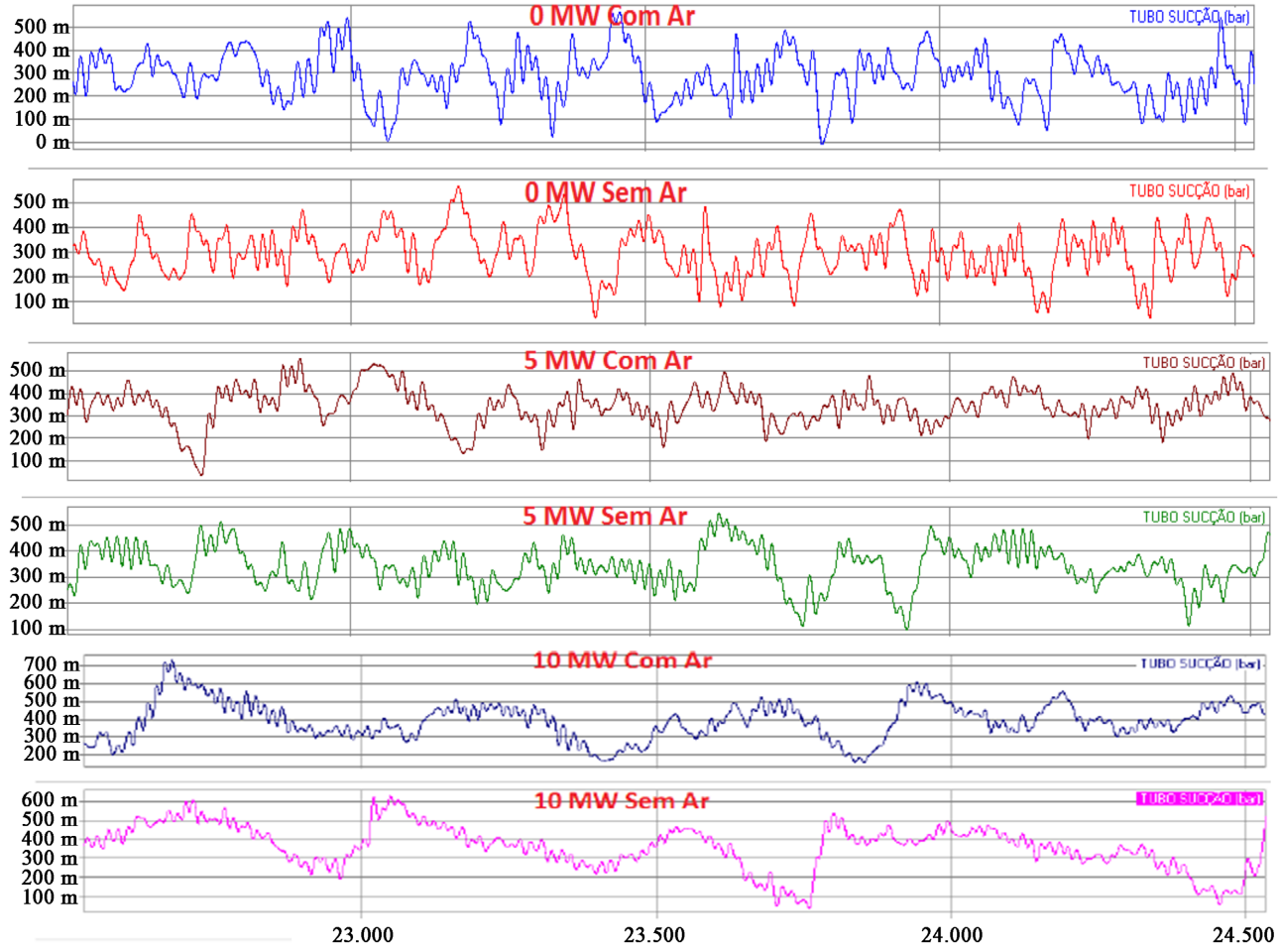

Figure B4. Suction Tube—Pressure oscillation measurements with 0, 5 and 10 MW.

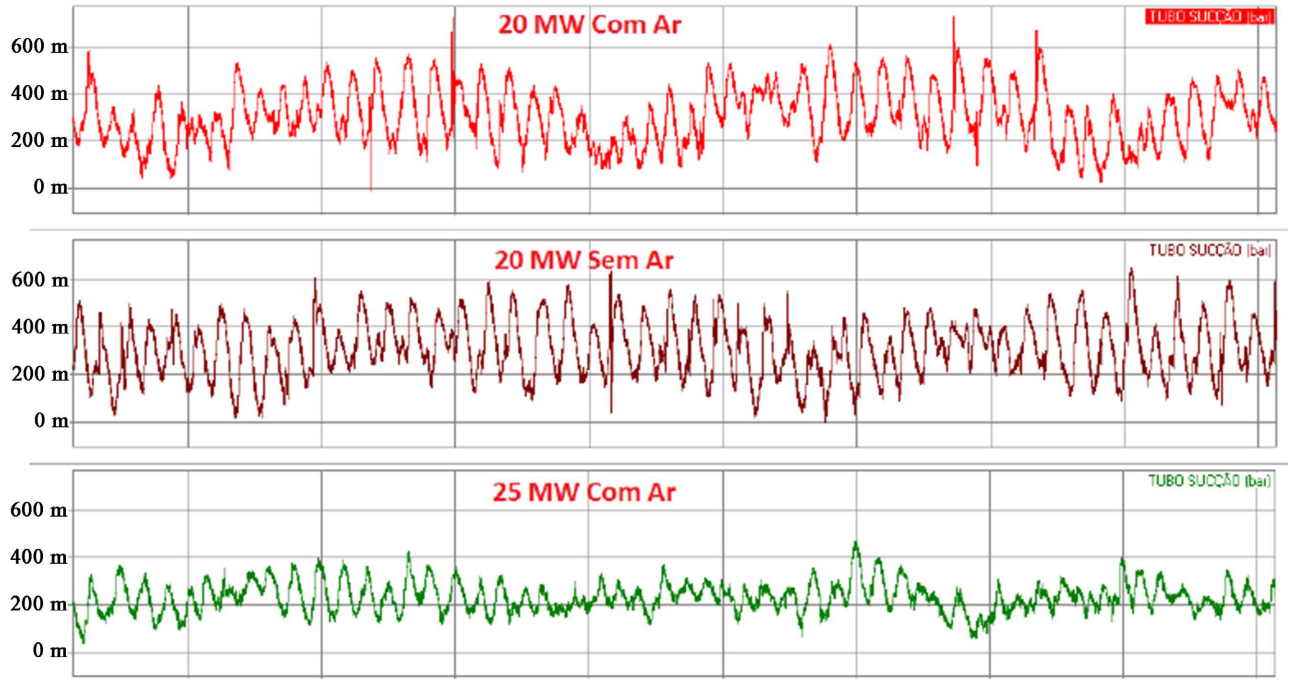

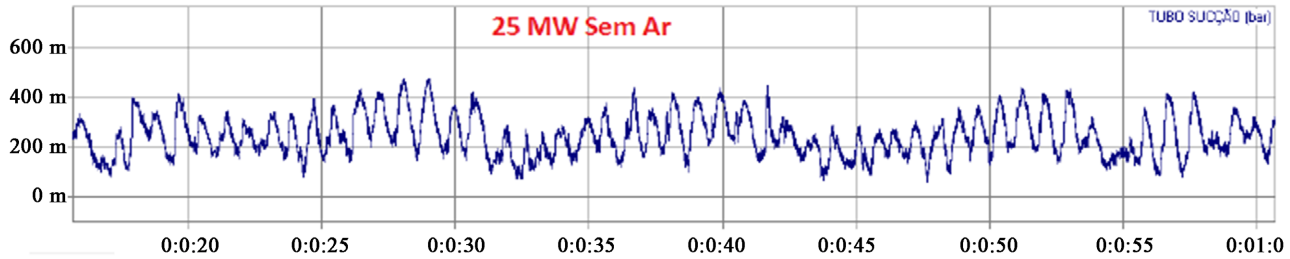

Figure B5. Suction Tube—Pressure oscillation measurements with 20 and 25 MW.

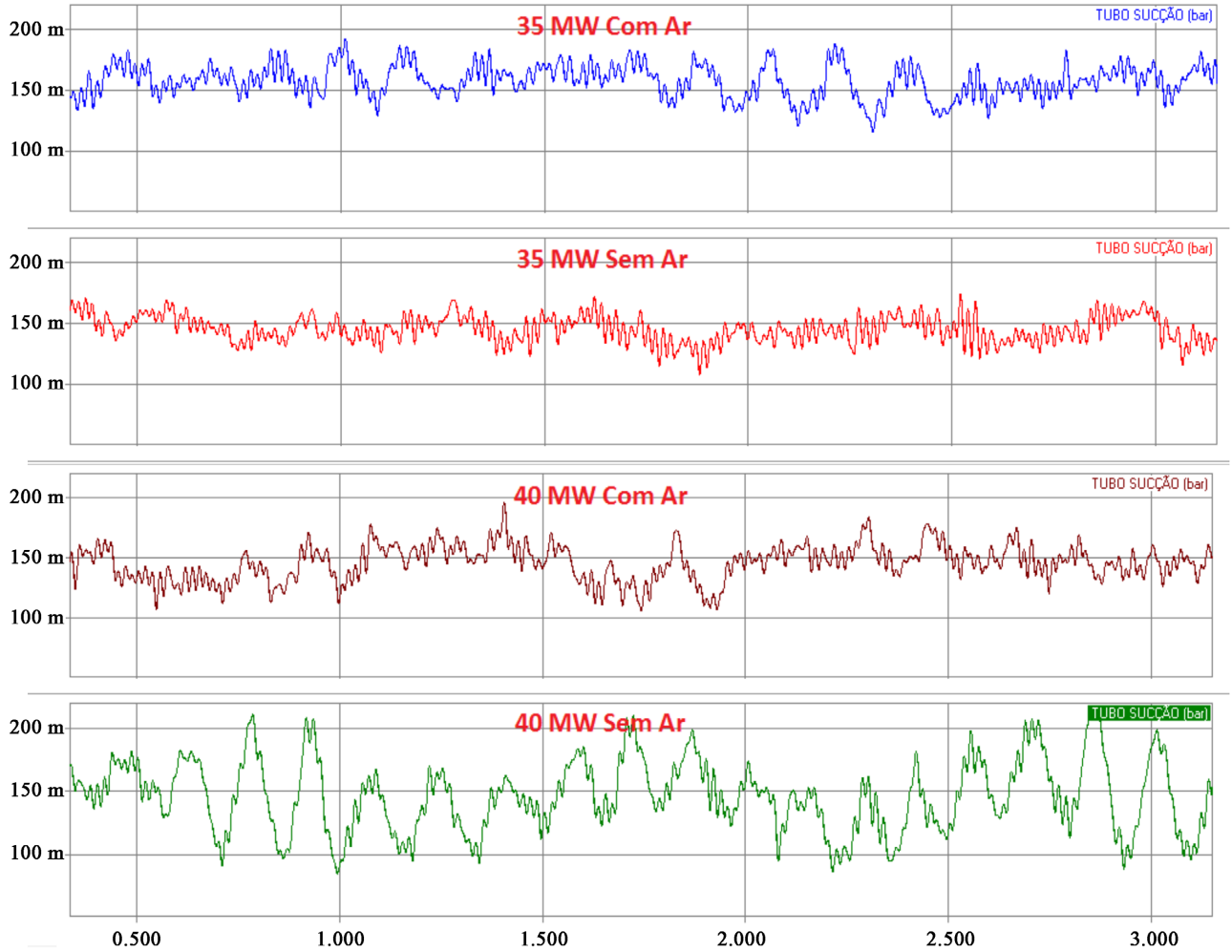

Figure B6. Suction Tube—Pressure oscillation measurements with 35 and 40 MW.

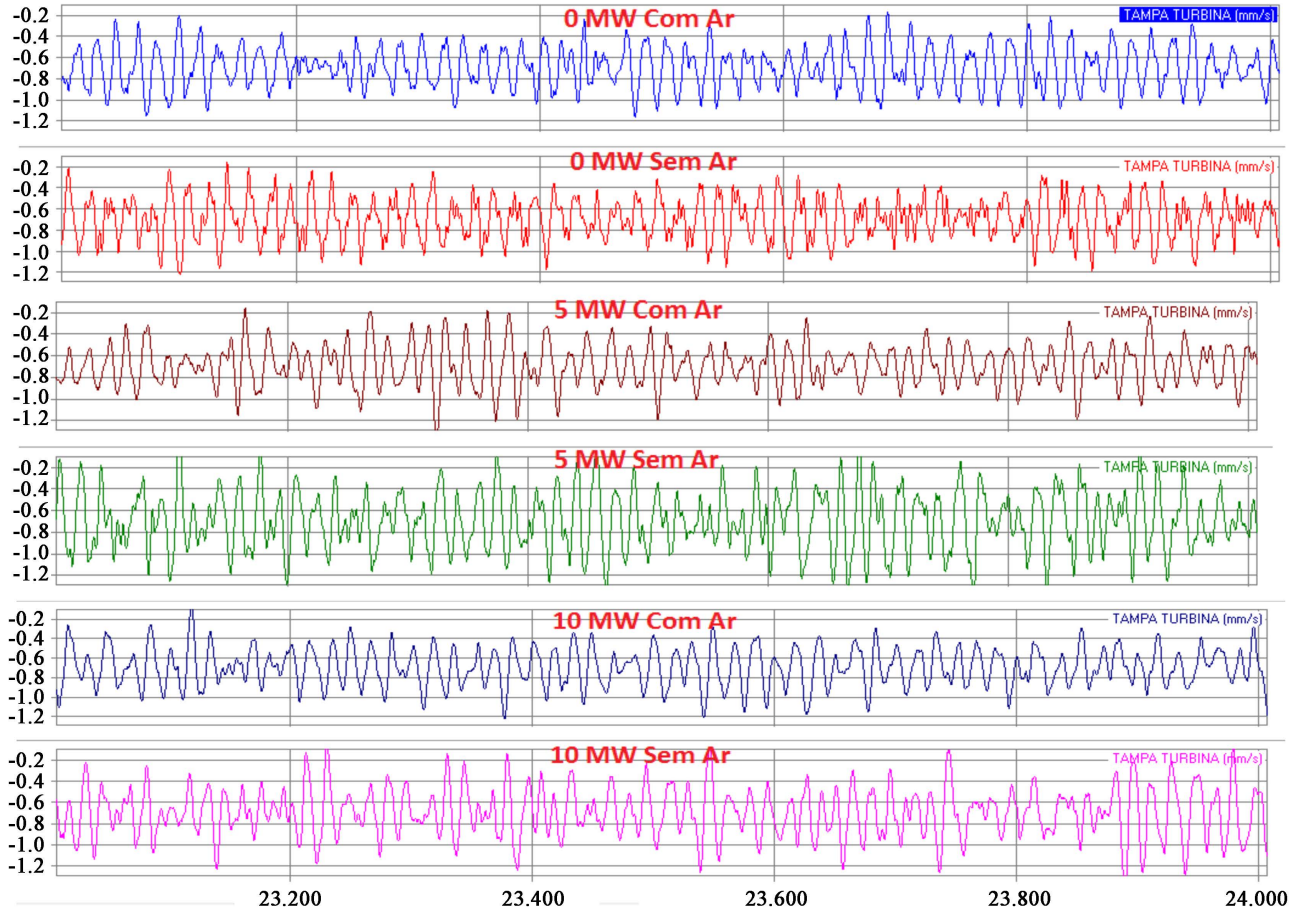

Figure B7. Turbine Cover—Vibration measurements with 0, 5 and 10 MW.

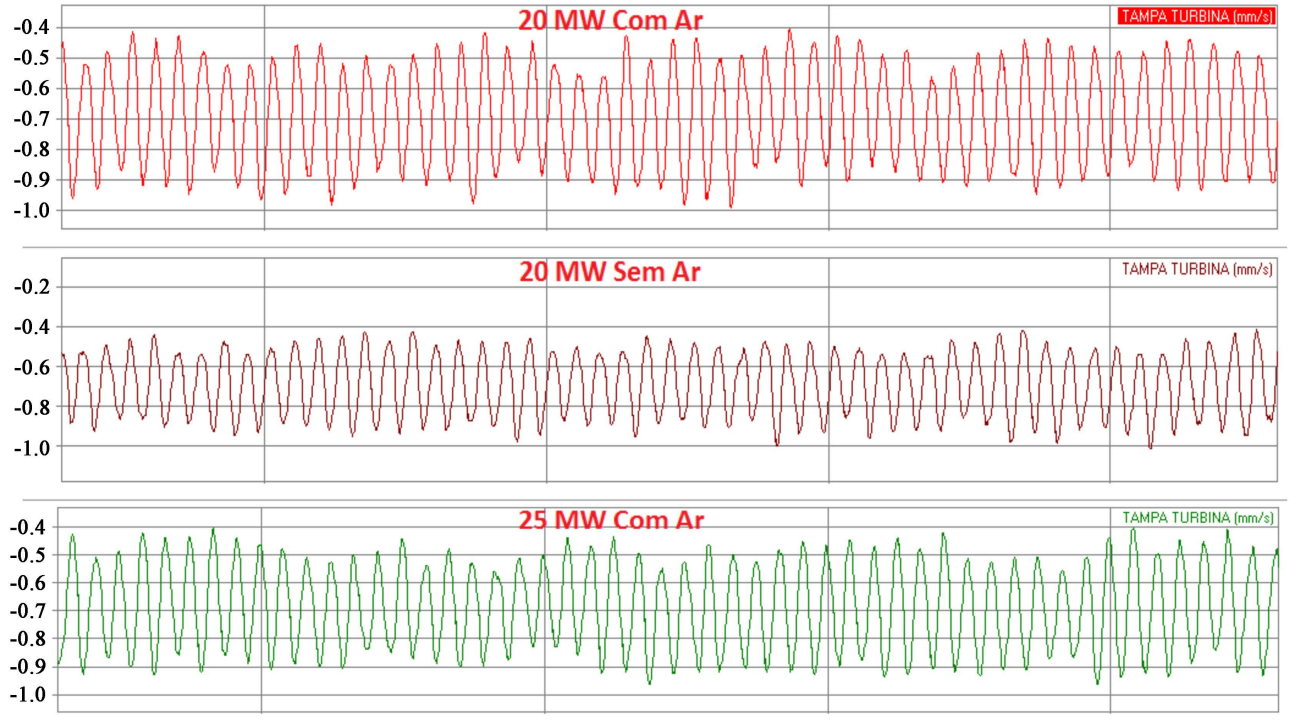

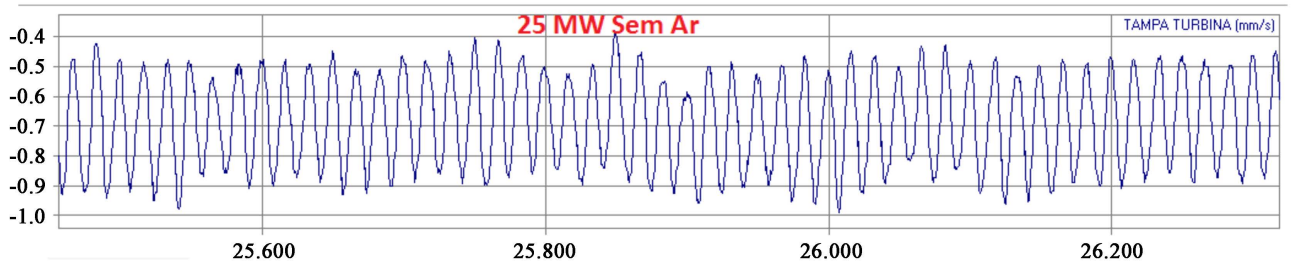

Figure B8. Turbine Cover—Vibration measurements with 20 and 25 MW.

Figure B9. Turbine Cover—Vibration measurements with 35 and 40 MW.